Characterization and Separation of Platinum-Based Antineoplastic Drugs by Zwitterionic Hydrophilic Interaction Liquid Chromatography (HILIC)–Tandem Mass Spectrometry, and Its Application in Surface Wipe Sampling

Stefano Dugheri [1],*, Nicola Mucci [2], Enrico Mini [3], Donato Squillaci [2], Giorgio Marrubini [4], Gianluca Bartolucci [5], Elisabetta Bucaletti [2], Giovanni Cappelli [2], Lucia Trevisani [2] and Giulio Arcangeli [2]

[1] Industrial Hygiene and Toxicology Laboratory, Occupational Medicine Unit, Careggi University Hospital, 50134 Florence, Italy
[2] Department of Experimental and Clinical Medicine, University of Florence, 50134 Florence, Italy; nicola.mucci@unifi.it (N.M.); donato.squillaci@unifi.it (D.S.); elisabetta.bucaletti@unifi.it (E.B.); giovanni.cappelli@unifi.it (G.C.); lucia.trevisani@unifi.it (L.T.); giulio.arcangeli@unifi.it (G.A.)
[3] Department of Health Sciences, University of Florence, 50134 Florence, Italy; enrico.mini@unifi.it
[4] Department of Drug Sciences, University of Pavia, Via Taramelli 12, 27100 Pavia, Italy; giorgio.marrubini@unipv.it
[5] Department of Neurosciences, Psychology, Drug Research and Child Health, University of Florence, 50019 Sesto Fiorentino, Italy; gianluca.bartolucci@unifi.it
* Correspondence: stefano.dugheri@unifi.it

Abstract: Platinum-based antineoplastic drugs (PtADs) are among the most important and used families of chemotherapy drugs, which, even showing severe side effects and being hindered by drug resistance, are not likely to be replaced clinically any time soon. The growing interest in the occupational health community in antineoplastic drug (AD) surface contamination requires the development of increasingly fast and easy high-throughput monitoring methods, even considering the lack of harmonized legally binding regulation criteria. Thus, a wipe sampling method together with zwitterionic hydrophilic interaction liquid chromatography (HILIC-Z)–tandem mass spectrometry (MS/MS) analysis was developed for the simultaneous evaluation of oxaliplatin, cisplatin, and carboplatin surface contaminations. A design of experiments approach was used to optimize the chromatographic conditions. Limits of quantification ranging from 2 to 5 ng/mL were obtained from interday and intraday repetitions for oxaliplatin and carboplatin, and between 170 and 240 ng/mL for cisplatin. The wipe desorption procedure is equivalent to other AD sampling methods, enabling a fast sample preparation, with an LC-MS/MS analysis time of less than 7 min.

Keywords: platinum-based antineoplastic drugs; cisplatin; carboplatin; oxaliplatin; HILIC–Z; liquid chromatography–mass spectrometry; wipe sampling; design of experiments (DoE)

1. Introduction

During the last 50 years, oncology has gone through remarkable changes, resulting in transforming malignant germ-cell testicular tumors from highly fatal to nearly uniformly cured neoplasms [1,2]. Cisplatin (cis-[$PtCl_2(NH_3)_2$]), first synthesized in 1844 by Italian chemist Michele Peyrone [3,4], was introduced in clinical trials in the late 1970s [5]; this clinical landmark was rightfully attributed to the identification of its anticancer potential by Barnett Rosenberg in his experiments dating to 1965 [6–8]. Cisplatin was accepted for pharmacological use in 1978, and since then, 25 platin drugs have entered clinical trials. Both the "second generation" and "third generation" of platinum-based antineoplastic drugs (PtADs), respectively, carboplatin, approved by the United States (US) Food and Drug Administration (FDA) as Paraplatin in 1989 [9], and oxaliplatin, authorized for clinical use in the European Union in 1999 and the US in 2002 [10], gained broadly worldwide

compliance. On the other hand, three other cisplatin analogs only obtained approval in single markets; nedaplatin in Japan, lobaplatin in China, and heptaplatin in Korea [11].

All the compounds belonging to this subfamily of ADs consist of a coordination complex containing a platinum atom in the oxidation state II or IV. The development of Pt-based drugs aimed to reduce toxicity, increase compound stability, and extend the application to different kinds of cancer. Among all the molecules synthesized and evaluated, carboplatin, thanks to its broader therapeutic index and reduced toxicity, was particularly interesting. Moreover, the greater stability of carboplatin is given by the chelating (cyclobutanedicarboxylate) ligand.

However, under chlorine-rich conditions, this second generation of compounds undergoes substitution of the carboxylate group, leading to cisplatin formation. Additionally, because of their similarity, it is inactive against cisplatin-resistant cancer. Thus, the third generation of platinum compounds, such as oxaliplatin, is characterized by greater stability due to the presence of two bidentate ligands. Therefore, to avoid the formation of highly reactive products (mono- or dichloro-platinum complexes), the presence of chloride ions is not recommended [10,12,13].

Regarding their action on deoxyribonucleic acid (DNA), the PtADs are DNA-interactive agents. They are classified as alkylating agents due to the ability of Pt^{2+} to coordinate double helix guanines [14]. Today, 50–70% of all patients are treated with platinum ADs [15–17]; in 2017, about 71% of the PtAD prescriptions were oxaliplatin [18], primarily for the treatment of colorectal cancers [12], while for the treatment of various solid tumors, cisplatin is still prescribed, and carboplatin is mainly used in the treatment of ovarian cancers [19]. The 2019–2029 worldwide market for PtADs is expected to grow at a compound annual growth rate (CAGR) of roughly 4.5%, driven by the rapidly increasing occurrence of cancers. The Asia Pacific market is the most expansive and fastest-growing region in the platinum-based AD market and is expected to grow with a 17% CAGR through to 2029 [20], evaluated at USD 1500 million in 2023 [21,22].

Despite their success, PtADs cause severe side effects, due to their indiscriminate attack on all high dividing rate cells, and they allow cancers to develop drug resistance [23]. Cisplatin is recognized as probably carcinogenic to humans in the List of Group 2A Agents by the International Agency for Research on Cancer (IARC) [24]. Addressing the toxicity of these drugs has been an ongoing challenge for clinicians and, more recently, for the occupational health community. Adverse reproductive effects on female healthcare workers and exposure to ADs have been correlated and described in a meta-analysis of 14 studies performed from 1966–2004 [25–27].

Over the past five years, the National Institute for Occupational Safety and Health (NIOSH), the American Conference of Governmental Industrial Hygienists (ACGIH), and the European Union have highlighted the importance of AD monitoring [28–30], with growing interest in surface contamination, which recently led the European Biosafety Network to publish a document in which a threshold value of 100 pg/cm^2 of surface contamination is recommended for ADs [31].

Regarding cytotoxic ADs, a simple way to indirectly assess dermal occupational exposure lies in monitoring surface contamination, usually carried out by wipe tests [32,33]. Since the AD handling process confers a very high risk of occupational exposure [34], appropriate use of safety cabinets, closed system transfer devices, and personal protective equipment (PPE) are highly recommended. Furthermore, during the handling process, the higher risk of exposure to antineoplastic agents is related to the hands; thus, among the various PPE types, medical gloves are the most relevant [35].

For the reasons described above, implementation of AD monitoring methods is required in all pharmaceutical fields, from human exposure to drug development, including formulation quality control, elimination in wastewater, and therapeutic drug surveillance. Inductively coupled plasma–mass spectrometry (ICP-MS) provides an excellent limit of quantification (LOQ) for the quantification of metal species, i.e., Pt can be observed in the

range of 0.1 to 1 ng/mL [36]. However, analyte speciation is achievable only by coupling with LC techniques [37].

Due to PtADs' low absorbance and high instability, the development of the LC-UV method is problematic. In fact, it suffers from poor sensitivity (a few µg/mL) [38–40]. The addition of a derivatization step improved sensitivity by up to two orders of magnitude [41,42]. Molecular MS has emerged in the last decade as a major tool to characterize metallodrug speciation [43]. More sensitive LOQs, between 2 and 25 ng/mL, were reached with LC-MS but only for single PtAD determination and often through derivatization [41,44,45].

Simultaneous analysis of cis-, carbo-, and oxaliplatin by liquid chromatography–tandem mass spectrometry (LC-MS/MS) by triple quadrupole has not yet been proposed.

In recent decades, an alternative strategy for the LC analysis of polar compounds has been found in hydrophilic interaction chromatography (HILIC) [46]. Andrew Alpert suggested that during the separation process, the hydrophilic analytes are partitioned between a water-enriched layer adsorbed on the surface of the stationary phase and a more hydrophobic mobile phase [47]. Depending on the triad compound functional groups, mobile phase composition, and stationary phase chemistry, different retention mechanisms, including strong electrostatic, dipole–dipole interactions, adsorption, and formation of hydrogen bonds [48], are thought to contribute together to the overall retention [49,50]. In addition, the dominating mechanism is influenced by many interacting factors such as the ionic strength and pH of the mobile phase that can be modulated by the addition of salts, acids and bases, buffers, type of organic solvent, and temperature [51,52]. These factors make the development of HILIC methods the ideal basis for applying chemometric tools such as design of experiments (DoE) and multivariate modeling. However, over the years, only a few researchers adopted these techniques for studying HILIC retention mechanisms and method development [53].

In the present study, we report on a shell particle–zwitterionic–HILIC LC-MS/MS method developed and validated to determine oxaliplatin, cisplatin, and carboplatin. Our method, coupled with the known technique of wipe sampling, provides a robust and rapid procedure for assessing PtAD surface contamination and personnel exposure in the hospital environment.

2. Materials and Methods

2.1. Chemicals

Ultra-high-performance liquid chromatography/mass spectrometry (UHPLC/MS) grade acetonitrile, water, and methanol absolute were all purchased from Biosolve Chimie SARL (Dieuze, France). Formic acid 99% LC/MS grade (Prod. Co. 405824) was purchased from Carlo Erba reagents (Milan, Italy). Ammonium hydroxide solution 30–33% (CAT n. 60-002-99) was purchased from Honeywell Fluka™ (Basel, Switzerland). Formic acid ammonium salt $\geq$ 99.0% MS grade (CAT n. 516961), toluene $\geq$ 99.9% high-performance liquid chromatography (HPLC) grade (CAT n. 650579), and daunorubicin hydrochloride $\geq$ 90% HPLC grade (CAS n. 23541-50-6, CAT n. 30450)—selected as internal standard (IS)—and carboplatin (CAS n. 41575-94-4, CAT n. C2538), cisplatin (CAS n. 15663-27-1, CAT n. C2210000), and oxaliplatin (CAS n. 61825-94-3, CAT n. O9512)—selected as chemical standards—were all purchased from Merck KGaA (Darmstadt, Germany).

The desorption solution (DS), consisting of a mixture of methanol:water 50:50 (v/v), was used to elute the wipe samples [32].

Pharmaceutical preparations of carboplatin 10 mg/mL, cisplatin 1 mg/mL, and oxaliplatin 5 mg/mL were purchased from Teva Pharmaceutical Industries Ltd (Petah Tiqwa, Israel).

2.2. Instruments

The LC system consists of a Shimadzu Nexera X2 equipped with a DGU-20A5R degasser unit, two LC-30AD pumps, SIL-30AC autosampler, a CBM-20A system controller,

SPD-M20A diode array detector, and CTO-20AC column oven. The used tandem mass spectrometry system was a Shimadzu LCMS 8050 triple quadrupole equipped with an electrospray source (ESI) [54]. Instrument control and data acquisition were carried out using the software LabSolution® ver. 5.97 (Shimadzu Corp., Kyoto, Japan).

Mobile phase pH was measured through a Hanna® Instruments portable pH meter mod. HI8424, equipped with an HI1230B pH electrode and an HI7662temperature probe.

Climatic Cabinet Sartorius SCC400L was used to weigh the IS, chemical standards, and ammonium formate salt.

2.3. Standard Solutions and Calibration Levels

Stock solutions of carboplatin, oxaliplatin, and daunorubicin (IS) were prepared at 1 mg/mL using the DS mixture, while cisplatin was prepared at the same concentration using water. All the stock solutions were stored at −20 °C. Diluted solutions of carboplatin, cisplatin, oxaliplatin, and IS were prepared from the stock solutions up to a concentration of 2 μg/mL in DS and used to optimize MS parameters.

The calibration mixture of analytes (MixPt solution) was prepared by adding aliquots of the pharmaceutical preparations by Teva (reported in Section 2.1) to obtain a 1 μg/mL concentration for carboplatin and oxaliplatin and 40 μg/mL for cisplatin. The IS working solution was made by diluting IS stock solution with a DS mixture up to 1 μg/mL.

A seven-level calibration curve for each analyte was prepared by adding 10 μL of IS working solution and proper volumes of MixPt, and diluted with DS mixture to reach a final volume of 1 mL. By following this procedure, the analyte concentrations of the calibration solutions were: 0, 5, 10, 20, 30, 40, 50 ng/mL for carboplatin and oxaliplatin, and 0, 200, 400, 800, 1200, 1600, 2000 ng/mL for cisplatin. Three levels of internal quality control (CQI) solutions were prepared by diluting MixPt with the DS mixture, to obtain 4 ng/mL (low level), 25 ng/mL (medium level), and 45 ng/mL (high level) for carboplatin and oxaliplatin, and 160 ng/mL (low level), 1000 ng/mL (medium level), and 1800 ng/mL (high level) for cisplatin. Each CQI solution contained IS in a concentration of 10 ng/mL.

The experimental design study for optimizing the chromatographic method was performed using the freshly prepared highest calibration.

2.4. Sample Preparation

Three sets of six replicates of samples were prepared to evaluate the matrix effect (ME) and the recovery (RE) for each analyte [55]. Set1 was obtained by adding 100 μL of the MixPt solution directly to a wipe cartridge [32], letting it dry for 10 min at room temperature, and desorbing it with 1.99 mL DS mixture. Set2 was made by desorbing the blank wipe cartridge with 2 mL of DS mixture, transferring 1.89 mL of this solution to a vial, and adding 100 μL of MixPt. Finally, Set3 was prepared by diluting 100 μL of MixPt solution with 1.89 mL of DS mixture. To each vial, 10 μL of IS working solution was added.

A solution of 5 mg/mL toluene in DS mixture was prepared to evaluate the void volume and the volume of the water layer adsorbed on the stationary phase. Each injected solution was filtered through a 0.2 μm GHP Acrodisc® syringe filter before analysis (Pall Corporation).

The method was tested in an actual sampling procedure inside an antineoplastic drug preparation unit after consistent use of PtADs. Wipe samples were prepared and collected, according to Dugheri et al. [32], at the beginning and the end of the work shift. Each collection consisted of 29 sampling points, chosen among the most likely contaminated surfaces.

2.5. Experimental Design

All computations were performed using the Chemometric Agile Tool (CAT, open source, free, developed from R, The R Foundation for Statistical Computing, available at https://www.r-project.org/, accessed on 22 March 2021) [56].

2.6. Chromatography and Instrument Parameters

Concerning the chromatography, an Agilent Poroshell 120® HILIC-Z 2.1 · 100 mm 2.7 μm particle size (Agilent Technologies, Santa Clara, CA, USA) (S.N. USHXF02517) column was used. The mobile phase consisted of a mixture of acetonitrile and water, with organic modifier ranging from 85% to 90%, at various ammonium formate concentrations and different pH values. The pH of the mobile phase was adjusted with formic acid or with ammonium hydroxide. Finally, the mobile phases were sonicated for 15 min to clear dissolved gasses from the solution and avoid gas bubbles in the LC pumps. The eluent was delivered isocratically at a flow rate of 0.6 mL/min, in a total run time of 5.5 min.

The void time of analysis and thus the retention factor (k) were assessed by estimating the water layer adsorbed on the surface of HILIC-Z stationary phase. For this purpose, a 5 mg/mL toluene solution was analyzed under two different elution conditions: firstly, utilizing an isocratic flow of pure acetonitrile, and secondly applying the optimized multiple reaction monitoring (MRM) analysis mobile phase as the solvent, which was acetonitrile 90%, H_2O 10% with 20 mM ammonium formate. Ten injections for each condition were repeated to establish the difference between the retention times of the analyte in acetonitrile ($t_{R(ACN)}$) and the mobile phase ($t_{R(Phase)}$). Toluene was detected at a wavelength of 254 nm by a photodiode array (PDA) detector. The water layer volume (V_w) and the volume ratio (β) were then calculated according to Guo et al. [57] through the following equations:

$$V_W = \left(t_{R(ACN)} - t_{R(Phase)} \right) \times F, \ \beta = \frac{V_W}{V_{Phase}} = \frac{V_{ACN}}{V_{Phase} - 1}.$$

Sample injection was carried out using a co-injection pretreatment program. The pretreatment optimization was fulfilled by repeating 3 MRM runs of the high calibration standard level for each injection condition and evaluating its response in peak shape and column overload. Co-injection was tested by loading the injection loop with 3 mixed aliquots made with increasing volumes of the sample (between 1 and 5 μL) and 8 μL of acetonitrile each, with a total injection volume of 27 to 39 μL. The MS/MS experiment co-injection pretreatment program consisted in three drawings of 2 μL from the sample vial alternated with three drawings of 8 μL from another vial containing acetonitrile.

The column thermostat was set at a temperature of 30 °C. The settings of the ESI source, operating in positive ion mode, were the following: interface voltage 4 kV, nebulizing gas flow 3 L/min, heating gas flow 10 L/min, interface temperature 300 °C, desolvation temperature 526 °C, desolvation line temperature 250 °C, heat block temperature 400 °C, and drying gas flow 10 L/min.

2.7. MS/MS Experiments

Positive Q3 scan spectra of the 2 μg/mL solutions of analytes were acquired in a range from 300 to 500 *m/z* with a scan time of 0.100 s.

The product ion scan (PIS) spectra of the 2 μg/mL solutions of analytes were acquired to study the fragmentation of each molecule in an *m/z* range from 60 to 400 with a 0.100 s scan time and using 270 kPa of argon as collision gas. Each solution was analyzed via flow injection analysis by increasing collision energies (CEs): from 5 to 55 V for oxaliplatin and carboplatin and from 5 to 35 V for cisplatin. Each run was performed with 5 μL of sample injection and 0.5 μL/min of flow, with an acquisition time of 0.6 min. The collision breakdown curves, graphics that show the relative abundance of each fragment ion produced by the analytes as the function of increasing CE, were built using the relative intensity values of each signal present in the MS/MS spectra.

The LC-MS/MS analyses were performed in positive mode MRM using a dwell time of 109 msec. The transition ions and energies are reported in Table 1.

Table 1. Quantifier and qualifier ions for each analyte with the corresponding collision energy utilized under the optimized parameters set in MRM mode.

Compound	Precursor Ion (m/z)	Quantifier Ion (m/z) (CE (V))	Qualifier Ion (m/z) (CE (V))
IS	528.10	306.00 (-51.0)	362.90 (-16.0)
Oxaliplatin	398.05	306.05 (-28.0)	96.00 (-25.0)
Cisplatin	317.90	264.90 (-15.0)	300.70 (-15.0)
Carboplatin	372.10	294.00 (-18.0)	248.00 (-35.0)

2.8. Performance Evaluation of LC-MS/MS Methods

The method precision was assessed as intraday and interday repeatability (intermediate precision) by the relative standard deviation percent (RSD%) of replicate analysis of low, medium, and high CQI levels. The intraday repeatability was evaluated from six sets of calibration and CQI solutions processed in a single day. To assess the interday repeatability of the method, three groups of calibration and CQI solutions were freshly prepared and analyzed every day for six days. Calibration curves were obtained by plotting the peak area ratios (PARs) between the analyte and IS quantitation ions versus the nominal concentration of the calibration solution. A linear regression analysis was applied to obtain the best fitting function between the calibration points. Limits of detection and quantitation (LOD and LOQ) were calculated according to the International Council for Harmonisation (ICH) guidelines using the approach based on the standard error of the y-intercept and slope of the regression [58].

The accuracy was determined by the ratio between the determined and added amounts of analytes to CQI solutions and expressed as mean RE percent.

ME and RE were calculated for each analyte by comparing the mean results of Set1, Set2, and Set3 described according to the following formula:

$$ME\ (\%) = \frac{Set2}{Set3} \times 100,\ RE\ (\%) = \frac{Set1}{Set2} \times 100.$$

IS was added to Set1, Set2, and Set3 to check chromatographic and injection conditions but was not used to evaluate *ME* and *RE*.

3. Results

3.1. Experimental Design

The chromatographic method was initially studied by the conventional trial-and-error approach. After some days of experiments, however, the need for a systematic approach to find suitable conditions for the elution of the three target compounds became apparent. Therefore, a D-optimal design was adopted to exploit all the possible experiments already performed and add only the experiments necessary to compute a model for studying three responses, namely the retention time, the peak width, and the sensitivity (measured by the peak areas) of the detection of the three analytes [59,60].

Four factors were considered, as reported in Table 2. The factors selected were the content of organic in the mobile phase (ACN from 85 to 90%), the amount of ammonium formate (FA, from 5 to 20 mM), the pH of the aqueous mobile phase (3.0 to 7.0), and the column compartment temperature (from 10 to 30 °C). The model selected was the canonical full factorial 2^4 with two-term interactions. Therefore, eight experiments carried out by the heuristic approach could be used (experiments numbered from 1 to 8) to complete a balanced dataset, adding only seven experiments (experiments numbered from 9 to 15) as shown in Table 2. After computing the model, six additional independent experiments were carried out for model validation. The results obtained (reported in Table S1) showed that only the models describing retention and peak width were applicable, whereas the four factors did not significantly affect the detection sensitivity.

Table 2. Experimental plan with results.

Exp #	ACN (%)	FA (mM)	pH	T (°C)	acn	fa	ph	t	Rt_{Cis}	Rt_{Car}	Rt_{Oxa}	A_{Cis}	A_{Car}	A_{Oxa}	W_{Cis}	W_{Car}	W_{Oxa}
1	90	20	6.4	10	1.00	1.00	0.70	−1.00	1.26	4.91	2.05	5,751,938.7	108,964.2	17,722.3	0.291	0.328	0.305
2	85	20	6.4	30	−1.00	1.00	0.70	0.60	0.96	1.87	1.09	2,111,931.5	66,125.7	12,669.0	0.337	0.294	0.289
3	90	20	6.4	30	1.000	1.000	0.700	0.60	1.37	4.41	2.00	5,783,404.3	170,263.5	24,244.2	0.291	0.314	0.303
4	90	20	6.4	35	1.000	1.000	0.700	1.00	1.37	4.29	1.98	3,515,024.5	93,620.7	12,778.5	0.291	0.303	0.307
5	90	20	7.0	30	1.000	1.000	1.000	0.60	1.28	4.17	1.85	3,593,408.0	91,063.5	17,679.2	0.294	0.309	0.299
6	90	20	3.0	30	1.00	1.00	−1.00	0.60	1.26	3.38	1.68	2,239,067.0	47,102.7	10,162.7	0.292	0.317	0.302
7	90	10	6.4	30	1.00	−0.33	0.70	0.60	1.36	4.36	1.98	4,033,975.0	95,439.0	13,555.2	0.290	0.313	0.309
8	90	5	6.4	30	1.00	−1.00	0.70	0.60	1.35	4.13	1.93	6,614,980.8	161,016.7	20,305.5	0.289	0.319	0.304
9	85	5	3.0	10	−1.00	−1.00	−1.00	−1.00	0.92	1.84	1.10	2,303,289.0	93,517.5	83,870.0	0.287	0.291	0.288
10	90	5	3.0	10	1.00	−1.00	−1.00	−1.00	1.10	3.02	1.54	2,328,438.8	81,673.7	71,948.3	0.290	0.310	0.293
11	85	20	3.0	10	−1.00	1.00	−1.00	−1.00	0.91	1.84	1.08	1,695,481.2	58,536.2	59,897.0	0.290	0.291	0.288
12	85	5	6.8	10	−1.00	−1.00	0.90	−1.00	0.90	1.91	1.11	1,833,141.5	60,208.7	72,325.8	0.296	0.290	0.286
13	85	20	6.8	10	−1.00	1.00	0.90	−1.00	0.93	2.24	1.20	1,148,948.5	43,399.7	50,491.8	0.289	0.304	0.287
14	90	5	7.0	10	1.00	−1.00	1.00	−1.00	1.10	3.66	1.70	3,905,167.5	85,353.8	65,230.7	0.287	0.316	0.297
15	85	5	3.0	35	1.00	−1.00	−1.00	1.00	0.94	1.70	1.06	2,271,161.3	90,683.5	82,863.2	0.286	0.294	0.286

Legend: column titles with capital letters refer to factors and their actual experimental values; column titles with lowercase letters refer to the factors and their coded values; ACN, acn acetonitrile; FA, fa, ammonium formate; pH, ph; T, t, column temperature; Rt, retention time; A, peak area; W, peak width measured at half height of the peak. Subscripts: Cis, cis-Pt; Car, carbo-Pt; Oxa, oxali-Pt.

Regarding the retention times of the three analytes, the models computed (Supplementary Material, Table S1) show that the percent of ACN, of course, had a significant impact on retention (i.e., the higher the %ACN, the stronger the retention of the analytes and the longer the retention times). More surprisingly, pH also had a significant effect on the retention of the three analytes. Carboplatin was the more strongly retained when pH was raised from 3 to 7, whereas cisplatin retention was the least susceptible to the mobile phase pH variation. Although the effect of temperature on retention times was statistically non-significant and the corresponding coefficients in the model were numerically very small, the interaction between temperature and pH instead resulted in significant and important factors determining the analytes' retention times. In particular, the interaction contributed more to increasing retention when both temperature and pH were at their high levels (pH 7 and 30 °C) or their low levels (pH 3.0 and 10 °C).

Out of the three models studied for peak width, the only valid model computed was that of cisplatin. A possible explanation for this outcome is that cisplatin is the less retained analyte between the three, and thus the peak width is less affected by measurement uncertainty, resulting in smaller variance associated with the model coefficients. The peak width model for cisplatin showed that ACN% of the mobile phase, temperature, and their interaction were the more relevant effects, and also statistically significant. Narrower peak widths were obtained when the lower % of ACN (85%) and the lower temperature (10 °C) were applied. However, the ACN%–temperature interaction effect counteracted the former two (see Supplementary Table S1, note the signs of the model's coefficients).

After evaluating the results, the best compromise to obtain the maximum retention and narrower peaks for the three analytes was using a mobile phase containing 90% acetonitrile, 20 mM ammonium formate at pH 6.4, and keeping the column temperature at 30 °C.

3.2. Chromatographic Conditions

The best co-injection program obtained consisted in three drawings of 2 μL from the sample vial alternated by three drawings of 8 μL from another vial containing acetonitrile, with a total injection volume of 30 μL. The pretreatment co-injection program allowed an increase in the total sample injection volume from 1.5 μL to 6 μL without altering peak shape or causing column overload.

The chromatographic profiles obtained display a good resolution between the platin molecules and a partial overlapping between cisplatin and the IS, as shown in Figure 1. Table 3 reports the retention time values, peak width, theoretical plate number, and retention factor.

Table 3. The analytes' retention time (R_T), peak width ($Width_{1/2}$), tailing factor 5% (T_f), asymmetry factor 10% (A_f), and their relative standard deviation (RSD), the calculated plate number (N), and the retention factor (k).

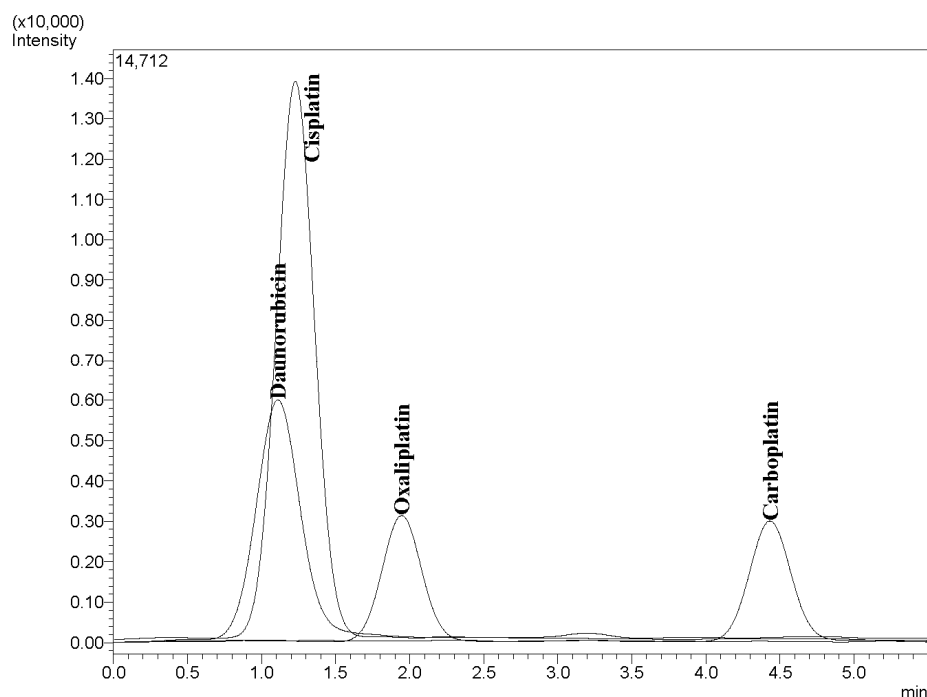| Compound	R_T (min)	R_T RSD	$Width_{1/2}$ (min)	Width RSD	T_f	T_f RSD	A_f	A_f RSD	N (plates)	k
Interday										
IS	1.12	2.0%	0.32	0.9%	1.06	0.7%	1.07	0.9%	68	1.21
Oxaliplatin	1.99	3.3%	0.30	0.7%	1.03	0.7%	1.04	0.8%	245	2.91
Cisplatin	1.23	1.7%	0.29	0.4%	1.02	1.7%	1.02	1.0%	101	1.43
Carboplatin	4.57	4.8%	0.31	0.7%	1.03	0.5%	1.05	0.6%	1182	7.98
Intraday										
IS	1.09	0.4%	0.32	0.5%	1.06	0.8%	1.07	1.2%	64	1.14
Oxaliplatin	1.89	0.2%	0.30	0.5%	1.03	2.3%	1.05	2.7%	227	2.72
Cisplatin	1.20	0.2%	0.29	0.3%	1.01	0.3%	1.02	0.4%	95	1.37
Carboplatin	4.26	0.1%	0.31	1.0%	1.03	2.4%	1.05	3.0%	1035	7.38

Figure 1. Platinum-based AD chromatogram.

The data in Table 3 (see also the chromatogram in Figure 1) evidence that the separation between the three platinum-containing analytes is complete. Although cisplatin co-elutes with the IS, this is not an issue since the MS detection perfectly discriminates the two analytes. The analysis takes only about five minutes, and the precision of all chromatographic parameters (retention times, peak width, tailing factor, asymmetry factor) is satisfactory. The figure for the number of theoretical plates (N) is reported to document the column efficiency of the method at the time of its initial development. The data can be used (and were used) to build control charts to monitor the column efficiency in routine applications. The retention factors within the interval of 1 < k < 10 were judged to be suitable for the goals of the separation based on the laboratory's internal expertise.

Since the water layer adsorbed on the column particles is part of the stationary phase, the toluene retention time observed in the analysis conditions ($t_{R(Phase)}$) can be considered the void time of analysis and is thus used to calculate the retention factor. Table S2 in the Supplementary Materials section reports the observed values for $t_{R(Phase)}$, $t_{R(ACN)}$, V_w, and β.

3.3. Mass Spectrometry

The most abundant signal of the unmodified molecule cluster was chosen as the parent ion for the MS/MS analysis, $[M + H]^+ = 398.05$ m/z for oxaliplatin, $[M + H]^+ = 372.1$ m/z for carboplatin, and $[M + NH_4]^+ = 317.9$ m/z for cisplatin. Collision breakdown curves were created for each molecule with the data obtained from PIS analysis and are reported in Figure 2. The analysis of these data allowed for selecting the most suitable product ions and their optimal CE to set up the respective MRM methods.
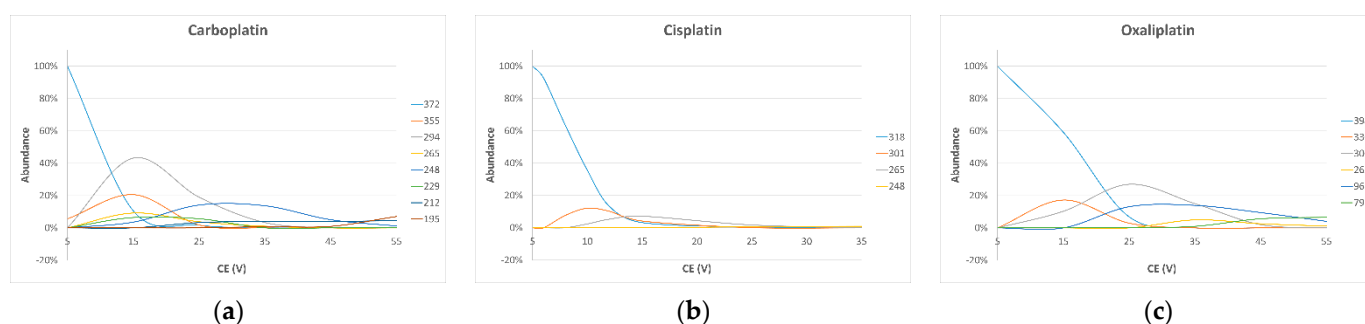
Figure 2. Collision breakdown curves obtained from PIS analysis reporting CE (V) versus percentage abundance. Each panel shows an analyte: (**a**) cisplatin; (**b**) carboplatin; (**c**) oxaliplatin.

3.4. Method Performance Evaluation

3.4.1. Calibration Curves

Pharmaceutical preparations have been used instead of pure standards to create the calibration curves to obtain a more accurate view of the compound's response, i.e., one that takes account of excipients which may cause a significant variability in the analyte signal.

Table S3 reports the obtained linear regression data LOD and LOQ values for each analyte for interday and intraday repetitions.

3.4.2. Matrix Effect and Recovery

Table S4 shows the results for ME and RE experiments. The values for ME $\geq$ 81% and RE $\geq$ 74% are satisfactory for the present study's aims.

3.4.3. Accuracy and Precision

Table S5 reports accuracy and precision figures of merit achieved for the three CQI levels during validation. The obtained precision (RSD between 3 and 9%) and accuracy (ratio between 91 and 111%) only show margins of error exceeding 10% for concentrations close to the LOQ. In the frame of the present study, these results were thus considered acceptable.

3.5. In-Field Method Application

From a panel of 58 samples, 4 end-shift wipes showed contamination inside the laminar flow hood (LFH). A scheme of the positive results is shown in Table S6 in the Supplementary Materials. Cisplatin contamination was detectable but lower than the LOQ limit.

4. Discussion

The analytical methods for biological monitoring of ADs that are currently available are not sensitive or specific enough for platinum-based compounds [61]. Consequently, the best choice to evaluate occupational exposure is surface monitoring. A wipe test is a widely used method in industrial hygiene and, currently, the only one able to detect ADs at levels as low as pg/cm^2. Healthcare workers' exposition risk depends on AD toxicity and how these drugs enter the body; this should guide their handling protocols.

The necessity to improve the sensitivity and quantification of polar compounds has led to the increased utilization of HILIC combined with ESI-MS detection. The acetonitrile-rich mobile phases employed in HILIC provide favorable conditions for efficient droplet formation and desolvation within the MS source. The zwitterionic (sulfoalkylbetaine) stationary phases contain both negatively charged sulfonate groups and positively charged quaternary ammonium groups in an equimolar ratio, separated by a short alkyl spacer. The sulfobetaine phase retains water strongly, allowing for creating an enriched water layer on its surface even at a high acetonitrile content in the mobile phase, which plays a critical role in retaining polar compounds [62–64]. Unfortunately, at the same time, the reconstitution of the thick water layer requires a long time after a gradient run. This last

issue led to the exclusion of the gradient elution, which would have made the analysis time extremely long, favoring the isocratic one. This choice, even if causing broader peaks and low retention for less well-retained molecules, allowed both good separation and a symmetric peak shape, along with short times for analysis. No carry-over effect or pressure rise caused by column contamination was observed during the analysis.

From earlier studies [32], to obtain a correct wipe desorption, a 50:50 water:methanol solution is needed to extract both hydrophilic and hydrophobic ADs. With the future perspective of unifying the studied molecules with other AD classes, this desorbing solution has been chosen for this study even if the hydrophilicity of PtADs would have suggested a higher water percentage. However, both ways would have led to chromatographic issues caused by the high water quantity in the injection volume. This would result in a poor peak shape, along with the possible loss of retention of the less well-retained substances. This issue could be resolved with injection volumes greater than 1.5 μL. The problem was solved thanks to the co-injection program (described in Section 3.2) possible with the SIL-30AC autosampler to modify the pretreatment program and mix the sample, right inside the injection loop, with minor amounts of acetonitrile present in another vial. This way, the autosampler works as a sample preparation unit, balancing the percentage of organic solvent in the injected solution and increasing the injection sample volume from 1.5 to 6 μL without affecting the chromatography. The loop capacity, in this case, 50 μL, must be considered when creating a co-injection method, since larger volumes would be excessive and thus partially discharged.

Though the simple suction of 6 μL of sample and 24 μL of acetonitrile at once would have required a faster pretreatment, the "sandwich-like" modality (2 + 8 μL · three times) is preferable because it allows better mixing of sample and solvent before the injection. In both ways, the pretreatment program increases the total time of analysis by 40 s per sample at most. It is essential to ensure that the decreasing percentage of water in the mixture does not lead to precipitation of the compounds inside the sample loop and cause obstructions in the column.

For what concerns the MS development, platinum-based compounds are undoubtedly challenging molecules. PtADs, especially cisplatin, are easily subjected to modifications and addition of molecules of water and acetonitrile to the coordination complex [63], which leads to the presence of many signals in the positive scan analysis of each pure standard. Furthermore, the natural occurrence of five stable isotopes of platinum, ^{192}Pt, ^{194}Pt, ^{195}Pt, ^{196}Pt, and ^{198}Pt, leads to peculiar isotopic clusters, also complicating the setup of MS/MS methods.

After fragmentation studies and selection of the optimal transitions to set MRM analysis, the obtained abundances for carboplatin and oxaliplatin allowed us to use a range of concentrations between 5 and 50 ng/mL due to their steady coordination structure. At the same time, cisplatin's low signal intensity required higher levels of the drug to create an acceptable calibration curve (200–2000 ng/mL).

The LODs and LOQs obtained are comparable to those found in the literature range of ng/mL—even if it is difficult to compare them since sample matrixes are different [44,45].

ME and RE results showed that wipe sampling is a suitable option for PtAD surface monitoring. These results show that a small percentage of the drug is retained from the wipe matrix, but the recoveries are still encouraging for a high-throughput monitoring plan.

As reported in Table S5 in the Supplementary Materials, the method has good repeatability, precision, and accuracy in the interday and intraday repetitions, with a larger variability—still under 15%—only in proximity to the LOQ concentrations.

The analysis of the wipe samples from the AD preparation unit showed a modest contamination inside the laminar flow hood which, in agreement with previous results [33], is one of the surfaces with a higher risk of contamination.

5. Conclusions

The inclusion of cisplatin in the group list of probably cancerogenic to human agents (2A) by the International Agency for Research on Cancer and the risk of toxicity due to dermal absorption concerning all PtADs require the development of an analytical method able to identify and quantify the target analytes to assess surface contamination. Herein is reported the development and optimization through a chemometric model of the LC-MS/MS method for the simultaneous separation and quantification of carboplatin, cisplatin, and oxaliplatin at the ng/mL level. The separation of the analytes was performed using a solid-core zwitterionic–HILIC column. Reliable qualitative and quantitative analysis can be performed with a fast and simple sample preparation and run time shorter than 7 min. The pretreatment co-injection program allowed us to increase the injection volumes without altering the chromatographic profile of the substances and improving method sensibility. The DoE approach permitted a substantial reduction of the number of tests needed for the method's development. Despite the molecular instability of platinum-based complexes, the obtained results showed adequate precision and accuracy. The present LC-MS/MS method can thus be proposed as a high-throughput procedure for surface contamination monitoring of PtADs.

Supplementary Materials: The following are available online at https://www.mdpi.com/article/10.3390/separations8050069/s1, Table S1. Models coefficients computed and validation studied on six independent replicates of experiments in the point with coded coordinates (1, 1, 0.7, 0.6) corresponding to the experimental conditions selected for the analyses, i.e., mobile phase containing ACN 90% (v/v), ammonium formate 20 mM, pH 6.4, and column temperature set at 30 °C. Table S2: Shows the observed values from which was calculated the column volume ratio in the chromatography operating conditions. Table S3. Linear regressions data, R^2, LOD, and LOQ of each analyte. Table S4. Data results for matrix effect (ME) and recovery (RE). Table S5. Data results of precision and accuracy for the three CQI levels. Table S6. A simple scheme of positive results due to PtADs contamination on Laminar Flow Hood (LFH) surfaces in pg/cm^2.

Author Contributions: Conceptualization, S.D., D.S. and E.B.; methodology and validation, D.S., E.B., G.C. and L.T.; formal analysis, G.M. and G.B.; investigation, G.C.; resources, N.M. and L.T.; data curation, G.M. and G.B.; writing—original draft preparation, S.D., D.S. and E.B.; writing—review and editing, N.M. and G.A.; visualization, E.M. and G.A.; supervision, E.M. and G.A.; project administration, G.A. All authors have read and agreed to the published version of the manuscript.

Conflicts of Interest: The authors declare no conflict of interest.

References

1. Hanna, N.; Einhorn, L.H. Testicular Cancer: A Reflection on 50 Years of Discovery. *J. Clin. Oncol.* **2014**, *32*, 3085–3092. [CrossRef]
2. Muggia, F.M.; Bonetti, A.; Hoeschele, J.D.; Rozencweig, M.; Howell, S.B. Platinum Antitumor Complexes: 50 Years Since Barnett Rosenberg's Discovery. *J. Clin. Oncol.* **2015**, *33*, 4219–4226. [CrossRef] [PubMed]
3. Peyrone, M. Ueber die Einwirkung des Ammoniaks auf Platinchlorür. *Eur. J. Org. Chem.* **1844**, *51*, 1–29. [CrossRef]
4. Alderden, R.A.; Hall, M.D.; Hambley, T.W. The Discovery and Development of Cisplatin. *J. Chem. Educ.* **2006**, *83*, 728–734. [CrossRef]
5. Esteban-Fernández, D.; Moreno-Gordaliza, E.; Cañas, B.; Palacios, M.A.; Gómez-Gómez, M.M. Analytical methodologies for metallomics studies of antitumor Pt-containing drugs. *Metallomics* **2010**, *2*, 19–38. [CrossRef] [PubMed]
6. Rosenberg, B.; Van Camp, L.; Krigas, T. Inhibition of Cell Division in Escherichia coli by Electrolysis Products from a Platinum Electrode. *Nat. Cell Biol.* **1965**, *205*, 698–699. [CrossRef] [PubMed]
7. Rosenberg, B.H.; Vancamp, L.; Trosko, J.E.; Mansour, V.H. Platinum Compounds: A New Class of Potent Antitumour Agents. *Nature* **1969**, *222*, 385–386. [CrossRef]
8. Kauffman, G.B.; Pentimalli, R.; Doldi, S.; Hall, M.D. Michele Peyrone (1813–1883), Discoverer of Cisplatin. *Platin. Met. Rev.* **2010**, *54*, 250–256. [CrossRef]
9. Dabrowiak, J.C. Platinum Anticancer Drugs. In *Metals in Medicine*; John Wiley & Sons Ltd: Chichester, UK, 2009; p. 109.
10. Graham, J.; Muhsin, M.; Kirkpatrick, P. Oxaliplatin. *Nat. Rev. Drug Discov.* **2004**, *3*, 11–12. [CrossRef]
11. Wheate, N.J.; Walker, S.; Craig, G.E.; Oun, R. The status of platinum anticancer drugs in the clinic and in clinical trials. *Dalton Trans.* **2010**, *39*, 8113–8127. [CrossRef]

12. Guichard, N.; Guillarme, D.; Bonnabry, P.; Fleury-Souverain, S. Antineoplastic drugs and their analysis: A state of the art review. *Analyst* **2017**, *142*, 2273–2321. [CrossRef] [PubMed]

13. Di Pasqua, A.J.; Kerwood, D.J.; Shi, Y.; Goodisman, J.; Dabrowiak, J.C. Stability of carboplatin and oxaliplatin in their infusion solutions is due to self-association. *Dalton Trans.* **2011**, *40*, 4821–4825. [CrossRef] [PubMed]

14. Wang, D.; Lippard, S.J. Cellular processing of platinum anticancer drugs. *Nat. Rev. Drug Discov.* **2005**, *4*, 307–320. [CrossRef]

15. Dyson, P.J.; Sava, G. Metal-based antitumour drugs in the post genomic era. *Dalton Trans.* **2006**, *16*, 1929–1933. [CrossRef]

16. Harper, B.W.; Krause-Heuer, A.M.; Grant, M.P.; Manohar, M.; Garbutcheon-Singh, K.B.; Aldrich-Wright, J.R. Advances in Platinum Chemotherapeutics. *Chem. A Eur. J.* **2010**, *16*, 7064–7077. [CrossRef]

17. Zalba, S.; Garrido, M.J. Liposomes, a promising strategy for clinical application of platinum derivatives. *Expert Opin. Drug Deliv.* **2013**, *10*, 829–844. [CrossRef]

18. Global Platinum Based Cancer Drug Market 2019 by Manufacturers, Regions, Type and Application, Forecast To 2024. Available online: https://www.360researchreports.com/global-platinum-based-cancer-drug-market-13860767 (accessed on 11 January 2021).

19. Rizvi, I.; Celli, J.P.; Evans, C.L.; Abu-Yousif, A.O.; Muzikansky, A.; Pogue, B.W.; Finkelstein, D.; Hasan, T. Synergistic Enhancement of Carboplatin Efficacy with Photodynamic Therapy in a Three-Dimensional Model for Micrometastatic Ovarian Cancer. *Cancer Res.* **2010**, *70*, 9319–9328. [CrossRef] [PubMed]

20. Platinum Cancer Drugs Global Market Is Expected to Grow with A CAGR of 17% in Forecast Period 2018–2029. Available online: https://www.medgadget.com/2019/12/platinum-cancer-drugs-global-market-is-expected-to-grow-with-a-cagr-of-17-in-forecast-period-2018-2029.html (accessed on 11 January 2021).

21. Global Platinum based Cancer Drug Market 2018 by Manufacturers, Regions, Type and Application, Forecast to 2023. Available online: https://www.fiormarkets.com/report/global-platinum-based-cancer-drug-market-2018-by-293950.html (accessed on 11 January 2021).

22. Global Platinum Based Cancer Drugs Market Share, Size, Trends, Industry Analysis Report by Drug Type (Cisplatin, Oxaliplatin, Carboplatin, Other), By Application (Colorectal Cancer, Ovarian Cancer, Lung Cancer, Other); By Regions, and Segment Forecast, 2019–2026. Available online: https://www.polarismarketresearch.com/industry-analysis/platinum-based-cancer-drugs-market) (accessed on 11 January 2021).

23. Ruggiero, A.; Trombatore, G.; Triarico, S.; Arena, R.; Ferrara, P.; Scalzone, M.; Pierri, F.; Riccardi, R. Platinum compounds in children with cancer: Toxicity and clinical management. *Anti-Cancer Drugs* **2013**, *24*, 1007–1019. [CrossRef]

24. Agents Classified by the IARC Monographs, Volumes 1–123. Last Update: 2 November 2018. Available online: https://monographs.iarc.fr/wp-content/uploads/2018/09/ClassificationsAlphaOrder.pdf (accessed on 11 January 2021).

25. Dranitsaris, G.; Johnston, M.; Poirier, S.; Schueller, T.; Milliken, D.; Green, E.; Zanke, B. Are health care providers who work with cancer drugs at an increased risk for toxic events? A systematic review and meta-analysis of the literature. *J. Oncol. Pharm. Pract.* **2005**, *11*, 69–78. [CrossRef]

26. Mahmoodi, M.; Soleyman-Jahi, S.; Zendehdel, K.; Mozdarani, H.; Azimi, C.; Farzanfar, F.; Safari, Z.; Mohagheghi, M.-A.; Khaleghian, M.; Divsalar, K.; et al. Chromosomal aberrations, sister chromatid exchanges, and micronuclei in lymphocytes of oncology department personnel handling anti-neoplastic drugs. *Drug Chem. Toxicol.* **2016**, *40*, 235–240. [CrossRef]

27. Villarini, M.; Gianfredi, V.; Levorato, S.; Vannini, S.; Salvatori, T.; Moretti, M. Occupational exposure to cytostatic/antineoplastic drugs and cytogenetic damage measured using the lymphocyte cytokinesis-block micronucleus assay: A systematic review of the literature and meta-analysis. *Mutat. Res.* **2016**, *770*, 35–45. [CrossRef]

28. Connor, T.H.; MacKenzie, B.A.; DeBord, D.G.; Trout, D.B.; O'Callaghan, J.P. *National Institute for Occupational Safety and Health List of Antineoplastic and Other Hazardous Drugs in Healthcare Settings*; US Department of Health and Human Services, Centers for Disease Control and Prevention, National Institute for Occupational Safety and Health: Cincinnati, OH, USA, 2016.

29. Directive 2004/37/EC of the European Parliament and of the Council of 29 April 2004 on the Protection of Workers from the Risks Related to Exposure to Carcinogens or Mutagens at Work (Sixth Individual Directive within the Meaning of Article 16(1) of Council Directive 89/391/EEC). Available online: https://eur-lex.europa.eu/LexUriServ/LexUriServ.do?uri=OJ:L:2004:229:0023:0034:EN:PDF (accessed on 11 January 2021).

30. European BioSafety Network, 2016, Preventing Occupational Exposure to Cytotoxic and Other Hazardous Drugs European Policy Recommendations. Available online: https://www.europeanbiosafetynetwork.eu/wp-content/uploads/2016/05/Exposure-to-Cytotoxic-Drugs_Recommendation_DINA4_10-03-16.pdf (accessed on 11 January 2021).

31. European BioSafety Network. 2019 Amendments to the Carcinogens and Mutagens Directive (CMD). The Network. 2019. Available online: https://www.europeanbiosafetynetwork.eu/wp-content/uploads/2019/03/Amendments-to-CMD3-and-implications.pdf (accessed on 11 January 2021).

32. Dugheri, S.; Bonari, A.; Pompilio, I.; Boccalon, P.; Mucci, N.; Arcangeli, G. A new approach to assessing occupational exposure to antineoplastic drugs in hospital environments. *Arch. Ind. Hyg. Toxicol.* **2018**, *69*, 226–237. [CrossRef] [PubMed]

33. Dugheri, S.; Bonari, A.; Pompilio, I.; Boccalon, P.; Tognoni, D.; Cecchi, M.; Ughi, M.; Mucci, N.; Arcangeli, G. Analytical strategies for assessing occupational exposure to antineoplastic drugs in healthcare workplaces. *Med. Pract.* **2018**, *69*, 589–603. [CrossRef]

34. Mucci, N.; Dugheri, S.; Farioli, A.; Garzaro, G.; Rapisarda, V.; Campagna, M.; Bonari, A.; Arcangeli, G. Occupational exposure to antineoplastic drugs in hospital environments: Potential risk associated with contact with cyclophosphamide- and ifosfamide-contaminated surfaces. *Med. Pract.* **2020**, *71*, 519–529. [CrossRef] [PubMed]

35. Oriyama, T.; Yamamoto, T.; Yanagihara, Y.; Nara, K.; Abe, T.; Nakajima, K.; Aoyama, T.; Suzuki, H. Prediction of the permeability of antineoplastic agents through nitrile medical gloves by zone classification based on their physicochemical properties. *J. Pharm. Health Care Sci.* **2020**, *6*, 23. [CrossRef]

36. Hann, S.; Lenz, K.; Stingeder, G. Novel separation method for highly sensitive speciation of cancerostatic platinum compounds by HPLC–ICP–MS. *Anal. Bioanal. Chem.* **2005**, *381*, 405–412. [CrossRef] [PubMed]

37. Hann, S.; Koellensperger, G.; Stefánka, Z.; Stingeder, G.; Fürhacker, M.; Buchberger, W.; Mader, R. Application of HPLC-ICP-MS to speciation of cisplatin and its degradation products in water containing different chloride concentrations and in human urine. *J. Anal. At. Spectrom.* **2003**, *18*, 1391–1395. [CrossRef]

38. Villarino, N.; Cox, S.; Yarbrough, J.; Martín-Jiménez, T. Determination of carboplatin in canine plasma by high-performance liquid chromatography. *Biomed. Chromatogr.* **2009**, *24*, 908–913. [CrossRef]

39. Burns, R.B.; Embree, L. Validation of high-performance liquid chromatographic assay methods for the analysis of carboplatin in plasma ultrafiltrate. *J. Chromatogr. B Biomed. Sci. Appl.* **2000**, *744*, 367–376. [CrossRef]

40. Toro-Córdova, A.; Ledezma-Gallegos, F.; Mondragon-Fuentes, L.; Jurado, R.; Medina, L.A.; Pérez-Rojas, J.M.; Garcia-Lopez, P. Determination of Liposomal Cisplatin by High-Performance Liquid Chromatography and Its Application in Pharmacokinetic Studies. *J. Chromatogr. Sci.* **2016**, *54*, 1016–1021. [CrossRef]

41. Shaik, A.N.; Altomare, D.A.; Lesko, L.J.; Trame, M.N. Development and validation of a LC–MS/MS assay for quantification of cisplatin in rat plasma and urine. *J. Chromatogr. B* **2017**, *1046*, 243–249. [CrossRef] [PubMed]

42. Bosch, M.E.; Sánchez, A.R.; Rojas, M.F.S.; Ojeda, C.B. Analytical methodologies for the determination of cisplatin. *J. Pharm. Biomed. Anal.* **2008**, *47*, 451–459. [CrossRef]

43. Wenzel, M.; Casini, A. Mass spectrometry as a powerful tool to study therapeutic metallodrugs speciation mechanisms: Current frontiers and perspectives. *Coord. Chem. Rev.* **2017**, *352*, 432–460. [CrossRef]

44. Desjardins, C.; Saxton, P.; Lu, S.X.; Li, X.; Rowbottom, C.; Wong, Y.N. A high-performance liquid chromatography–tandem mass spectrometry method for the clinical combination study of carboplatin and anti-tumor agent eribulin mesylate (E7389) in human plasma. *J. Chromatogr. B* **2008**, *875*, 373–382. [CrossRef] [PubMed]

45. Ito, H.; Yamaguchi, H.; Fujikawa, A.; Tanaka, N.; Furugen, A.; Miyamori, K.; Takahashi, N.; Ogura, J.; Kobayashi, M.; Yamada, T.; et al. A full validated hydrophilic interaction liquid chromatography–tandem mass spectrometric method for the quantification of oxaliplatin in human plasma ultrafiltrates. *J. Pharm. Biomed. Anal.* **2012**, *71*, 99–103. [CrossRef] [PubMed]

46. Linden, J.C.; Lawhead, C.L. Liquid chromatography of saccharides. *J. Chromatogr. A* **1975**, *105*, 125–133. [CrossRef]

47. Alpert, A.J. Hydrophilic-interaction chromatography for the separation of peptides, nucleic acids and other polar compounds. *J. Chromatogr. A* **1990**, *499*, 177–196. [CrossRef]

48. Yoshida, T. Peptide separation by Hydrophilic-Interaction Chromatography: A review. *J. Biochem. Biophys. Methods* **2004**, *60*, 265–280. [CrossRef]

49. Ikegami, T.; Tomomatsu, K.; Takubo, H.; Horie, K.; Tanaka, N. Separation efficiencies in hydrophilic interaction chromatography. *J. Chromatogr. A* **2008**, *1184*, 474–503. [CrossRef]

50. Wohlgemuth, J.; Karas, M.; Jiang, W.; Hendriks, R.; Andrecht, S. Enhanced glyco-profiling by specific glycopeptide enrichment and complementary monolithic nano-LC (ZIC-HILIC/RP18e)/ESI-MS analysis. *J. Sep. Sci.* **2010**, *33*, 880–890. [CrossRef]

51. Hemström, P.; Irgum, K. Hydrophilic interaction chromatography. *J. Sep. Sci.* **2006**, *29*, 1784–1821. [CrossRef]

52. Guo, Y.; Gaiki, S. Retention behavior of small polar compounds on polar stationary phases in hydrophilic interaction chromatography. *J. Chromatogr. A* **2005**, *1074*, 71–80. [CrossRef] [PubMed]

53. Taraji, M.; Haddad, P.R.; Amos, R.I.; Talebi, M.; Szucs, R.; Dolan, J.W.; Pohl, C.A. Chemometric-assisted method development in hydrophilic interaction liquid chromatography: A review. *Anal. Chim. Acta* **2018**, *1000*, 20–40. [CrossRef] [PubMed]

54. Fenn, J.B.; Mann, M.; Meng, C.K.; Wong, S.F.; Whitehouse, C.M. Electrospray ionization-principles and practice. *Mass Spectrom. Rev.* **1990**, *9*, 37–70. [CrossRef]

55. Matuszewski, B.K.; Constanzer, M.L.; Chavez-Eng, C.M. Strategies for the Assessment of Matrix Effect in Quantitative Bioanalytical Methods Based on HPLC−MS/MS. *Anal. Chem.* **2003**, *75*, 3019–3030. [CrossRef] [PubMed]

56. Leardi, R.; Melzi, C.; Polotti, G. CAT, Chemometric Agile Tool. Available online: http://gruppochemiometria.it/index.php/software (accessed on 22 March 2021).

57. Guo, Y.; Bhalodia, N.; Fattal, B.; Serris, I. Evaluating the Adsorbed Water Layer on Polar Stationary Phases for Hydrophilic Interaction Chromatography (HILIC). *Separations* **2019**, *6*, 19. [CrossRef]

58. VALIDATION OF ANALYTICAL PROCEDURES: TEXT AND METHODOLOGY Q2(R1). Available online: https://database.ich.org/sites/default/files/Q2%28R1%29%20Guideline.pdf (accessed on 18 March 2021).

59. Leardi, R. D-Optimal Designs. Chemometrics. In *Encyclopedia of Analytical Chemistry*; Myers, R., Ed.; John Wiley & Sons, Ltd.: Chichester, UK, 2018. [CrossRef]

60. Marrubini, G.; Dugheri, S.; Cappelli, G.; Arcangeli, G.; Mucci, N.; Appelblad, P.; Melzi, C.; Speltini, A. Experimental designs for solid-phase microextraction method development in bioanalysis: A review. *Anal. Chim. Acta* **2020**, *1119*, 77–100. [CrossRef]

61. Dugheri, S.; Bonari, A.; Pompilio, I.; Gentili, M.; Montalti, M.; Mucci, N.; Arcangeli, G. A new automated gas chromatography/solid phase microextraction procedure for determining α-fluoro-β-alanine in urine. *Malays. J. Anal. Sci.* **2017**, *21*, 1091–1100. [CrossRef]

62. Greco, G.; Grosse, S.; Letzel, T. Study of the retention behavior in zwitterionic hydrophilic interaction chromatography of isomeric hydroxy- and aminobenzoic acids. *J. Chromatogr. A* **2012**, *1235*, 60–67. [CrossRef]

63. McCalley, D.V.; Neue, U.D. Estimation of the extent of the water-rich layer associated with the silica surface in hydrophilic interaction chromatography. *J. Chromatogr. A* **2008**, *1192*, 225–229. [CrossRef]

64. Ehrsson, H.C.; Wallin, I.B.; Andersson, A.S.; Edlund, P.O. Cisplatin, Transplatin, and Their Hydrated Complexes: Separation and Identification Using Porous Graphitic Carbon and Electrospray Ionization Mass Spectrometry. *Anal. Chem.* **1995**, *67*, 3608–3611. [CrossRef]